



Research Article

Adsorption and Corrosion Mitigation Effect of Two New Salen-type Schiff Bases on Mild Steel in Acidic Medium: Experimental and Computational Studies

Wahab OO.^{1*}, Waziri I.², Zirra CS.¹, Onile AA.¹, Abdulsalami IO.¹, Garba S.³ and Olasunkanmi LO.⁴

¹Department of Chemistry, Faculty of Natural and Applied Sciences, Nigerian Army University Biu, Nigeria

²Department of Pure and Applied Chemistry, University of Maiduguri, P.M.B. 1069, Maiduguri, Nigeria

³Department of Chemistry, Faculty of Science, Nigerian Defence Academy, Kaduna, Kaduna State, Nigeria

⁴Department of Chemistry, Faculty of Science, Obafemi Awolowo University, Ile-Ife 220005, Nigeria

*Corresponding author: Email: olaide.wahab@naub.edu.ng, doi.org/10.55639/607.010000

ARTICLE INFO:

Keyword:

Corrosion,
DFT,
Inhibitor,
Monte-Carlo,
Salen Schiff bases

ABSTRACT

The quest for more green inhibitors for suppression of material corrosion continues to appreciate due to rising industrialization and advancement in technology. In this work, the abilities of two new salen-type Schiff bases: bis(3,5-dibromosalicylaldehyde) ethylenediamine (DBSE) and bis(3,5-dichlorosalicylaldehyde) ethylenediamine (DCSE) to suppress corrosion of mild steel in 1 M HCl solution were investigated by weight loss method, scanning electron microscopy (SEM), conceptual DFT calculation and molecular dynamics (Monte-Carlo) simulation. The results showed that these compounds are excellent suppressors of mild steel degradation in the acid solution as the degradation process was efficiently retarded to the tune of 92.9% and 97.5% by DCSE and DBSE, respectively at 500 μ M inhibitor concentration and 313 K. Suppression efficiency was found to increase with concentration and decrease at elevated temperature due to prevalence of desorption. Adsorption of the inhibitor molecules on mild steel surface occurred by physisorption and in compliance with the Temkin isotherm. The results of SEM analysis confirmed successful formation of protective layers of the inhibitor molecules on the steel surface. Interaction descriptors from DFT calculations and Monte Carlo simulations confirmed the observed ranking of suppression ability as DBSE > DCSE with suspected contributions from both the neutral and protonated forms of the Schiff bases. We conclude that both DCSE and DBSE can be deployed as efficient green inhibitors for the mitigation of mild steel corrosion especially at low to moderately high temperatures.

Corresponding author: Wahab O. O., Email: olaide.wahab@naub.edu.ng

Department of Chemistry, Faculty of Natural and Applied Sciences, Nigerian Army University Biu, Nigeria

INTRODUCTION

Corrosion, a spontaneous electrochemical process of degradation of metallic objects in aggressive environments is of global concern, owing to its severe adverse effects on life, economy, and environmental well-being. It drastically lowers the functionality, efficiency, durability, utility value and even the safety of materials.

The process of mitigating the effects of aggressive media on materials is termed corrosion inhibition. Various means of inhibiting material corrosion include surface treatments, coating, and the use of sacrificial anode, drying agents, or surface-active chemical substances called inhibitors (Abeng, *et al.*, 2017; Umoren & Solomon, 2017). However, the use of corrosion inhibitors (especially the organic inhibitors) is arguably the most widely used preventive approach because it is relatively inexpensive, straightforward, eco-friendly, readily available, effective over a good range of temperatures and compatible with varieties of materials (Brycki *et al.*, 2018).

A major disappointment with mild steel is its high susceptibility to corrosion even in mild corrosive environments. Consequently, industrial equipment, plants, pipelines, etc., which are frequently in contact with aggressive solutions, are vulnerable to deterioration. The use of inorganic inhibitors is steadily being discouraged due to toxicity and safety concerns. Organic inhibitors on the other hand are relatively less toxic and more environmentally compatible in addition to their higher economic affordability and greater availability. Consequently, various classes of organic inhibitors derived from oxazole, triazole, pyrazole, carbazole, imidazole, thiourea, amine, pyridine, flavonoid, coumarin and Schiff base frameworks have been investigated for corrosion mitigation potential (Assad & Kumar, 2021; Berisha, 2020; Boughoues *et al.*, 2020; El Ibrahim & Guo, 2020; Haque *et al.*, 2018; Jamil

et al., 2018; Li *et al.*, 2022; Mrani *et al.*, 2018; Nwankwo *et al.*, 2017; Olasunkanmi *et al.*, 2021; Olasunkanmi *et al.*, 2020; Resen *et al.*, 2021; Verma *et al.*, 2019; Verma & Quraishi, 2021; Zinad *et al.*, 2020). However, the Schiff base class (i.e. compounds characterized by presence of a C=N linkage) continues to attract attention and has remained the focus of most corrosion inhibition studies probably due to its synthetic simplicity, economic affordability, relatively lower toxicity, higher biocompatibility, good thermal stability and remarkable inhibition efficiency (%I.E).

Despite the enormity of research on anticorrosion activity of Schiff base compounds, studies on corrosion mitigation potential of the salen-type Schiff bases are scanty. This class of sparingly soluble Schiff base compounds are derived from combination of two salicylaldehyde units with a diamine, giving rise to four possible sites for coordination (i.e. two imine nitrogen and two hydroxyl oxygen) (Fig. 1) (Ebrahimi, Hadi, Abdulnabi, & Bolandnazar, 2014). Owing to their good chelating property, salen-type Schiff bases have mainly been deployed as ligands for the development of bioactive metal complexes (Es-Sounni *et al.*, 2022). However, some studies have shown that salen-type and related Schiff bases could effectively inhibit material corrosion (Da Silva *et al.*, 2010; Ravari *et al.*, 2009; Seifzadeh *et al.*, 2016).

Ravari *et al.* (2009) investigated the corrosion inhibition effects of two salen-type Schiff bases on copper in 0.5 M H₂SO₄ (Ravari *et al.*, 2009). The Schiff bases which were derived by combining hexylene diamine with salicylaldehyde (Compound A2) and methoxy-substituted salicylaldehyde (Compound A1) gave 85% and 90%, respectively, as the highest percentage inhibition. Adriana *et al.* (2010) studied the corrosion mitigation properties of N,N'-bis(salicylidene)-1,2-ethylenediamine and its reduced form, N,N'-bis(2-hydroxybenzyl)-

1,2-ethylenediamine for carbon steel protection in 1 M HCl solution (Da Silva *et al.*, 2010). In this study, the reduced form of the inhibitor was found to show higher protection performance than the unreduced form. Corrosion inhibition study by Seifzadeh and co-workers (Seifzadeh *et al.*, 2016) revealed that 5-CM-salophen Schiff base effectively mitigated the deterioration of mild steel in 0.5 M HCl solution. In a recent study by Nor and co-worker (2022), bis(5-bromosalicylaldehyde) ethylenediamine and its Mn(II) complex were found to exhibit an excellent inhibition effect on steel corrosion in 1 M HCl solution, with the complex performing slightly better than the free ligand (Nor Zaini *et al.*, 2022).

Given the scantiness of reports on the anticorrosion activity of salen-type Schiff bases, it is necessary to study more of these compounds to better understand their corrosion inhibition behaviour. It is with this view that the present study investigated the corrosion mitigation effects of two new salen-type Schiff bases: bis(3,5-dibromosalicylaldehyde) ethylenediamine (DBSE) and bis(3,5-dichlorosalicylaldehyde) ethylenediamine (DCSE) (Fig. 1) on mild steel corrosion in 1 M

HCl solution. These Schiff base compounds were synthesized by the condensation reaction of ethylenediamine with 3,5-dibromosalicylaldehyde and 3,5-dichlorosalicylaldehyde, respectively.

This study consists of experimental and computational parts where the experimental part covers synthesis, characterization, gravimetric measurement (using weight loss method), adsorption isotherms and surface morphological study using scanning electron microscopy (SEM). On the other hand, the computational part used the instruments of density functional theory (DFT) and molecular dynamics simulation to probe the experimentally observed corrosion inhibition activities of the synthesized compounds. DFT calculations were involved in this study to understand the nexus between the electronic structures of the Schiff bases and their corrosion mitigation activities. On the other hand, the essence of the molecular dynamics simulation is to obtain additional insights on the favorability of interaction between the Schiff bases and mild steel surface and also predict the interaction energy as well as possible changes in molecular configuration on the steel surface.

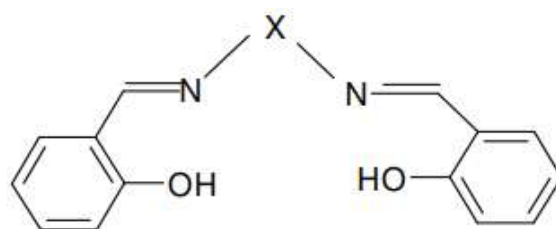


Figure 1: General molecular structure of salen-type Schiff base. X is hydrocarbon e.g. $(\text{CH}_2)_2$, $(\text{CH}_2)_3$, $(\text{CH}_2)_4$, $(\text{CH}_2)_5$, etc.

EXPERIMENTAL AND COMPUTATIONAL DETAILS

Chemicals and measurements

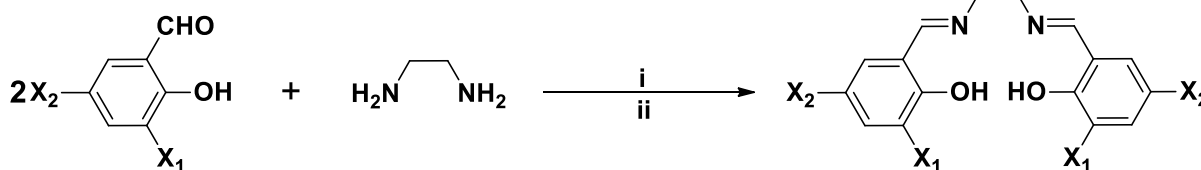
The chemicals and reagents used in this study were of analytical grade (AR), obtained from Merck Pvt. Ltd., and were used as received.

Elemental analyses (C, H, and N) were measured using VarioElementar III microbe CHN analyzer. Infrared spectra were recorded on a Bruker Tensor 27 and the Perkin-Elmer FT-IR spectrometer BX. The ^1H NMR spectra were obtained using a Bruker 500 MHz spectrometer,

while the $^{13}\text{C}\{\text{H}\}$ NMR spectra were obtained using a Bruker 125 MHz spectrometer. For ^1H NMR and $^{13}\text{C}\{\text{H}\}$ NMR spectra, the chemical shifts were referred to DMSO- d_6 at $\delta_{\text{H}} = 2.50$ and $\delta_{\text{C}} = 39.50$, respectively at room temperature. Electronic spectra were obtained on an UV-1900 Shimadzu UV-Visible spectrometer at room temperature. Powder X-ray diffraction analysis data were collected using a Rigaku miniFlex600 benchtop model with Cu-K α radiation ($\lambda = 1.5418 \text{ \AA}$) over 2θ range of $0\text{--}80^\circ$ at room temperature. Mass spectra were obtained using high resolution mass spectrometry on a WatersAcquity UPLC Synapt G2HD machine.

General procedure for the synthesis of the compounds

Schiff bases are usually synthesized by the classical condensation of a primary amine and an aldehyde or ketone (Waziri *et al.*, 2023). In



Scheme 1: General procedure for the synthesis of the compounds: i = $\text{CH}_3\text{OH}/\text{HCOOH}$, and ii = ambient temperature. **DCSE:** $\text{X}_1=\text{X}_2=\text{Cl}$; **DBSE:** $\text{X}_1=\text{X}_2=\text{Br}$.

Bis(3,5-dichlorosalicylaldehyde) ethylenediamine (DCSE)

Yield: (1.12 g, 83 %); yellow solid; m.p. $223\text{--}225^\circ\text{C}$; ^1H NMR (500 MHz, DMSO- d_6): δ (ppm) = 3.99 (s, 4H, $(\text{CH}_2)_2$), 7.46 (d, 2H, Ar-H, $J = 7.5$ Hz), 7.59 (d, Ar-H, $J = 8.0$ Hz), 8.60 (s, 2H, $(\text{HC}=\text{N})_2$), 14.08 (br, 2H, $(\text{OH})_2$); $^{13}\text{C}\{\text{H}\}$ NMR (125 MHz, DMSO- d_6): δ (ppm) = 166.3 (C-OH, Ar-C), 159.9 (HC=N), 133.3, 130.0, 123.1, 119.1, 118.1 (Ar-C), 55.4 (CH_2); Selected IR_{ATR} : (ν , cm^{-1}): 3047 (OH), 1632 (HC=N), 1306 (C-N), 1060 (C-O), 737 (C-Cl); UV-Visible (DMSO, 10^{-3}M): 274 nm; ($\pi\rightarrow\pi^*$), 352 nm; ($n\rightarrow\pi^*$); CHN Anal. Calculated for $\text{C}_{16}\text{H}_{12}\text{Cl}_4\text{N}_2\text{O}_2$; C, 47.32; H, 2.98; N, 6.90; found: C, 47.25; H, 2.90; N, 6.87; HRMS-ESI m/z $[\text{M}+\text{H}]^+ = 404.9543$ (Calculated for $\text{C}_{16}\text{H}_{12}\text{Cl}_4\text{N}_2\text{O}_2$, = 404.9731).

Bis(3,5-dibromosalicylaldehyde) ethylenediamine (DBSE)

Yield: (1.02 g, 76 %); light yellow solid; m.p. $246\text{--}250^\circ\text{C}$; ^1H NMR (500 MHz, DMSO- d_6): δ (ppm) = 3.99 (s, 4H, $(\text{CH}_2)_2$), 7.60 (d, 2H, Ar-H, $J = 9.5$ Hz), 7.79 (d, Ar-H, $J = 9.0$ Hz), 8.57 (s, 2H, $(\text{HC}=\text{N})_2$), 13.09 (br, 2H, $(\text{OH})_2$); $^{13}\text{C}\{\text{H}\}$ NMR (125 MHz, DMSO- d_6): δ (ppm) = 165.7 (C-OH, Ar-C), 160.9 (HC=N), 137.1, 133.1, 118.0, 113.2, 105.4 (Ar-C), 54.6 (CH_2); Selected IR_{ATR} : (ν , cm^{-1}): 3081 (OH), 2858 (C-H), 1635 (HC=N), 1335 (C-N), 1089 (C-O), 683 (C-Br); UV-Visible (DMSO, 10^{-3}M): 213 nm;

($\pi \rightarrow \pi^*$), 277 nm; ($\pi \rightarrow \pi^*$), 347 nm; ($n \rightarrow \pi^*$), CHN Anal. Calculated for $C_{16}H_{12}Br_4N_2O_2$; C, 32.91; H, 2.07; N, 4.80; found: C, 32.89; H, 2.05; N, 4.77; HRMS-ESI m/z $[M+H]^+ = 580.9680$ (Calculated for $C_{16}H_{12}Br_4N_2O_2$, = 580.7711).

Corrosion inhibition study

Surface pre-treatment of mild steel samples and preparation of corrosive media

Each mild steel (MS) coupon used for this experiment was of 1 cm by 4 cm dimension and is approximately composed of 99.074% Fe, 0.17% C, 0.46% Mn and trace amounts of Al, Si, P, Cr, Ni, and Cu (Olasunkanmi *et al.*, 2021). The MS was polished with abrasives of uniform grit, washed with water, degreased in acetone and then dried in a hot atmosphere. The corrosive 1 M HCl solution used as control (blank) was prepared from commercially obtained 37% HCl acid of analytical grade by diluting appropriate volume of the acid with distilled water. Inhibitor-treated corrosive media were prepared in varied concentrations of 100 μM - 500 μM in 1 M HCl. To enhance dissolution, DCSE and DBSE were first dissolved in 5 mL DMF and 5 mL ethanol,

$$CR = \frac{87.6W}{At} \quad (1)$$

$$\theta = \frac{CR_0 - CR_i}{CR_0} = 1 - \frac{CR_i}{CR_0} \quad (2)$$

$$IE\% = \theta \times 100 \quad (3)$$

where W is weight loss, A is the area of steel surface, t is immersion time, CR_0 is corrosion rate in the absence of inhibitor and CR_i is corrosion rate in the presence of inhibitor.

Surface morphology

To visually ascertain the inhibitors' interactions with mild steel surface for mitigation of mild steel corrosion, the surface morphology of the corroded steel samples from the blank and inhibited media were inspected with the aid of Phenom-ProX scanning electron microscope for only the experiment conducted at 313 K.

respectively before being made up to 1 L stock solution with 1 M HCl.

Gravimetric measurements

The gravimetric method is used to estimate corrosion rate, surface coverage and inhibition efficiency (IE%) based on loss in weight of mild steel when immersed in a corrosive medium. Pre-treated steel samples were weighed and immersed into 100 mL beakers containing blank and inhibitor-treated corrosive media in a thermostatic water bath at 313 K and 343 K. After immersion time of 3 hours, the steel samples were removed, washed with distilled water, degreased in acetone, dried in a hot atmosphere, and reweighed. Values of weight loss were determined, and corresponding corrosion rates (CR), surface coverage (θ) and inhibition efficiencies (IE%) were calculated using Equations 1-3 (Al-Baghdadi *et al.*, 2021; Verma *et al.*, 2016):

Adsorption mode and thermodynamics

Adsorption isotherms are important tools in corrosion inhibition studies as they help to determine the preferred mode of interaction (i.e. physical or chemical) of an inhibitor with metallic surfaces. This mode of interaction is probed in this study via isotherm plots of Langmuir, Temkin, Frumkin and Freundlich to determine the model that best describes the adsorption behavior of the studied inhibitors. Langmuir, Temkin, Frumkin and Freundlich adsorption models can be expressed as (Basiony *et al.*, 2019; Mrani *et al.*, 2018; Olasunkanmi *et al.*, 2021; Olasunkanmi *et al.*, 2020):

$$\frac{\theta}{1-\theta} = K_{ads}C_{inh} \quad (\text{Langmuir isotherm}) \quad (4)$$

$$\ln \frac{\theta}{c(1-\theta)} = \ln K_{ads} + 2\alpha\theta \quad (\text{Frumkin isotherm}) \quad (5)$$

$$\ln \theta = \left(\frac{1}{2\alpha}\right) \ln C_{inh} + \left(\frac{1}{2\alpha}\right) \ln K_{ads} \quad (\text{Temkin isotherm}) \quad (6)$$

$$\ln \theta = \frac{1}{n} \ln C_{inh} + \ln K_{ads} \quad (\text{Freundlich Isotherm}) \quad (7)$$

where θ is the surface coverage, C_{inh} is inhibitor concentration, K_{ads} is adsorption equilibrium constant, α is the maximum amount of adsorbate and a is the interaction parameter.

$$\Delta G_{ads}^{\circ} = -RT \ln(55.5K_{ads}) \quad (8)$$

where R and T are gas constant and absolute temperature, respectively. The numerical value 55.5 represents the molar concentration of water in acid solution.

Calculation of molecular electronic structure by Density functional theory (DFT)

This computational study was accomplished with Gaussian 09 program (M. Frisch *et al.*, 2009). The electronic structures of DCSE and DBSE were investigated by DFT calculations to unravel the impacts of their electronic properties on their corrosion mitigation activities, and to determine the dominant form (neutral or protonated) of each molecule that is responsible for interaction with mild steel in the corrosion inhibition set-up.

Well-constructed models of the neutral and protonated forms of the Schiff bases were fully optimized to their ground state minimum geometries in vacuum and simulated aqueous HCl medium at the wb97xd/6-311++G(d,p) level of theory (Chai *et al.*, 2008; Clark, *et*

$$\text{Energy gap } (\Delta) = E_{LUMO} - E_{HOMO} \quad (9)$$

$$\text{Global softness } (\sigma) = \frac{1}{\eta} = \frac{2}{(E_{LUMO} - E_{HOMO})} \quad (10)$$

$$\text{Chemical potential } (\Phi) = -\chi = \frac{1}{2}(E_{LUMO} + E_{HOMO}) \quad (11)$$

$$\text{Fractions of electrons transferred } (\Delta N) = \frac{\phi_{Fe} - \chi_{inh}}{2(\eta_{Fe} + \eta_{inh})} \quad (12)$$

Adsorption Gibb's free energy change (ΔG_{ads}) was calculated from K_{ads} according to the following relation (Basiony *et al.*, 2019; Olasunkanmi *et al.*, 2021; Olasunkanmi *et al.*, 2020):

al., 1983; Frisch, *et al.*, 1984). Calculations in simulated HCl solution were achieved with the integral equation formalism polarizable continuum model (IEFPCM) using dielectric constant values of 78.3 and 1.573 (as static and optical parameters, respectively) (Olasunkanmi *et al.*, 2021; Sulaiman & Onawole, 2016). All optimized molecular models were confirmed to be authentic by absence of imaginary vibrational frequency and all energy values were zero-point corrected.

The corrosion mitigation potentials of the compounds were assessed based on some quantum molecular descriptors which include energy gap (Δ), global softness (σ), chemical potential (Φ) and fractions of electrons transferred (ΔN). These were derived from the energies of frontier molecular orbitals (E_{HOMO} and E_{LUMO}) of the compounds according to the following relations (Olasunkanmi *et al.*, 2021; Wahab *et al.*, 2020):

where E_{HOMO} and E_{LUMO} are energies of the highest occupied molecular orbital and lowest unoccupied molecular orbital, η_{Fe} and ϕ_{Fe} symbolize the absolute hardness and work function of iron respectively while η_{inh} and χ_{inh} are the absolute hardness and electronegativity for inhibitor, respectively. Values of $\phi_{Fe} = 4.82$ eV/mol and $\eta_{Fe} = 3.59$ eV/mol used for ΔN computation in this work were adopted from Kokalj (2012) (Kokalj, 2012).

Monte-Carlo Simulation

Monte-Carlo (MC) simulation is a popular molecular dynamics method used for predicting the energetics of an inhibitor's interaction with mild steel surface as well as the configuration of the inhibitor after interaction with the surface.

Relative abilities of DBSE and DCSE to mitigate mild steel corrosion were compared based on their affinities for mild steel surface as reflected by their calculated adsorption energies. Mild steel, being mainly composed of iron was ably represented in this study by Fe (1 1 0) :

$$E_{ads} = -(E_{Inh/Fe110} - E_{Fe110} - E_{Inh}) \quad (13)$$

RESULTS AND DISCUSSION

Synthesis and Characterization

The reaction between ethylenediamine with dichloro and dibromo salicylaldehyde using methanol as a solvent in the presence of catalytic amount of formic acid, yielded the Schiff base compounds (DCSE and DBSE) (**Scheme 1**). The compounds were obtained in high yield (1.12 g, 83 % DCSE and 1.02 g, 76 % DBSE) and purity. The compounds were found to be soluble in methanol, ethanol, chloroform, acetone, dichloromethane, dimethyl sulfoxide, and dimethylformamide, and are air/light stable. Their formation was established using various spectroscopic techniques. The 1H and $^{13}C\{H\}$ NMR, FTIR data (in the supplementary

spleaved surface due to its unique stability and large concentration of Fe atoms on this surface (Anderson & Mehandru, 1984; Arya & Carter, 2004; Guo *et al.*, 2017).

Adsorption of a single molecule of DBSE and DCSE (i.e. the adsorbate) onto the Fe (1 1 0) surface (i.e. the adsorbent) was simulated by the Monte-Carlo approach using the adsorption locator module of the Acceryls Material Studio 2013 (Akkermans *et al.*, 2013). The simulation was set-up by loading the DFT-optimized structure of each inhibitor on the surface (within 10 Å distance from the surface) and invoking a simulated annealing task with COMPASS force field and smart algorithm. The simulation was carried out in 5 cycles at a *fine* accuracy level, with each cycle consisting of 50000 steps. This allowed the inhibitor molecule (adsorbate) assume a more stable configuration at a suitable location on the adsorbent surface. The adsorption energy was then calculated as (Nigussa)

information) of all the compounds are in good agreement with their proposed molecular structures. Furthermore, the mass spectroscopy of the compounds reveal single and stable molecular ion peaks on the spectrum correlating with the molecular weights of the compounds, supporting their purity and stability.

Gravimetric measurements

Effect of inhibitor concentration

The inhibition effect of DCSE and DBSE on mild steel corrosion in 1 M HCl was evaluated gravimetrically at 313 K and 343 K only. The corrosion rate (CR), surface coverage (θ) and inhibition efficiency (IE%) derived from weight loss (W) of steel after immersion time of 3 hr are listed in Table 1. As can be observed from this

table, corrosion mitigation efficiency increases with inhibitor concentration and attained maximum values of 92.9% and 97.5% at 500 μM of DCSE and DBSE, respectively, and 313 K. These IE% values are indicative of a good corrosion inhibitor. The drastic fall in IE% observed at 343 K suggests that only a small portion of the inhibitor molecules could adsorb successfully onto the surface of mild steel at elevated temperature due to increased disorderliness. This is explained in the next section.

DBSE showed higher surface protection efficiency than DCSE probably because it occupied a relatively larger area on the metal surface as a result of its bigger size compared to DCSE (Olasunkanmi *et al.*, 2021). Beside the nitrogen atom of the imine function, other constituents of the inhibitor molecules suspected to be responsible for their corrosion mitigation behaviour include the oxygen atom of the hydroxyl group, the halogen substituents, and the π -conjugated phenyl rings.

Table 1: Loss in weight of mild steel, corrosion rate, surface coverage and inhibition efficiency obtained in 1 M HCl without and with various concentrations of DCSE and DBSE at 313 K and 343 K.

T(K)	Conc. (μM)	W (g)		CR ($\text{g cm}^{-2} \text{h}^{-1}$)		Θ		IE%	
		DCSE	DBSE	DCSE	DBSE	DCSE	DBSE	DCSE	DBSE
313	Blank	0.084		0.613		---	---	---	---
	100	0.052	0.033	0.380	0.241	0.381	0.651	38.1	65.1
	200	0.037	0.022	0.270	0.161	0.560	0.737	56.0	73.7
	300	0.035	0.017	0.256	0.124	0.583	0.798	58.3	79.8
	400	0.024	0.013	0.175	0.095	0.714	0.845	71.4	84.5
	500	0.006	0.002	0.044	0.015	0.929	0.975	92.9	97.5
343	Blank	0.860		6.278		---	---	---	---
	100	0.760	0.599	5.548	4.373	0.116	0.303	11.6	30.3
	200	0.651	0.462	4.752	3.373	0.243	0.463	24.3	46.3
	300	0.630	0.432	4.599	3.154	0.267	0.498	26.7	49.8
	400	0.592	0.388	4.322	2.832	0.312	0.549	31.2	54.9
	500	0.570	0.334	4.161	2.438	0.337	0.612	33.7	61.2

Comparing the synthesized Schiff bases with some existing Schiff bases that have been assessed for corrosion inhibition activity, the data given in Table 2 show that the relative

performances of the synthesized Schiff bases as inhibitors of mild steel corrosion in acidic medium are highly comparable to those reported in the literature

Table 2: Comparative performance of the studied Schiff bases with other Schiff bases reported in literature.

Schiff base	Corrosive medium	%IE at 500 μ M and 30 $^{\circ}$ C/40 $^{\circ}$ C	Reference
Aniline derivatives	1 M H ₂ SO ₄	92.42% - 99.02%	(Chitra, <i>et al.</i> , 2010)
Quinoline derivative	1 M HCl	91%	(Lgaz <i>et al.</i> , 2016)
Quinazolinone derivatives	1 M HCl	92% - 96%	(Jamil <i>et al.</i> , 2018)
Tetrahydropyridines derivatives	1 M HCl	84.59% - 91.89%	(Haque <i>et al.</i> , 2018)
Gallic acid derivatives	0.5 M HCl	90%	(Basiony <i>et al.</i> , 2019)
Coumarin derivative	1 M HCl	95.1%	(Zinad <i>et al.</i> , 2020)
Semicarbazide and p-toluidine derived Schiff bases	1 M HCl	79% and 86%	(Olasunkanmi <i>et al.</i> , 2020)
Hydrazine carboxamides	1 M HCl	82% without KI, 97% with KI	(Olasunkanmi <i>et al.</i> , 2021)
Pyrrole derivative	1 M HCl	94.5%	(Al-Baghdadi <i>et al.</i> , 2021)
Piperazine derivative	1 M HCl	93.42%	(Resen <i>et al.</i> , 2021)
2-Pyridine carboxaldehyde derivative	1 M HCl	93.93% - 94.04%	(Li <i>et al.</i> , 2022)
Bis(3,5-dibromosalicylaldehyde) ethylenediamine	1 M HCl	97.6%	This work
Bis(3,5-dichlorosalicylaldehyde) ethylenediamine	1 M HCl	92.8%	This work

Effect of temperature

The effect of temperature on the inhibition efficiency of DCSE is very evident in Table 1. A 30 degree rise in temperature from 313 K to 343 K led to a drastic reduction in surface coverage, a dramatic increase in corrosion rate and weight loss, and a consequent lowering of IE%. At the lower temperature (i.e. 313 K), the relatively smaller agitation in the system appeared to favour adsorption more than desorption of the inhibitor molecules since the equilibrium is more posited towards adsorption. However, increasing the temperature to a higher value (343 K) shifted the equilibrium position towards

desorption thereby resulting in the detachment of already adsorbed molecules from the metal surface due to increased agitation (Olasunkanmi *et al.*, 2021; Olasunkanmi *et al.*, 2020). This explains the lower inhibition efficiency observed at 343 K compared to 313 K.

Since IE% decreases with an increase in temperature, physisorption is suspected as the prevalent mode of adsorption of the inhibitor molecules, as explained elsewhere (Chitra *et al.*, 2010).

The temperature dependence of CR can be expressed in concurrence with the Arrhenius equation as (Eddy *et al.*, 2008):

$$\ln\left(\frac{CR_2}{CR_1}\right) = \frac{E_a}{R}\left(\frac{1}{T_1} - \frac{1}{T_2}\right) \quad (21)$$

where CR_2 and CR_1 are the corrosion rates obtained at temperatures T_1 and T_2 which are 313 K and 343 K, respectively, R is the gas

constant and E_a is the activation energy. The calculated values of E_a at varying concentrations of the inhibitors are presented in Table 3.

Table 3: Activation energies at various concentrations of DCSE and DBSE

Conc. (μM)	E_a (kJ/mol)	
	DCSE	DBSE
Blank	69.33	
100	79.89	86.37
200	85.46	90.65
300	86.07	96.43
400	95.56	101.16
500	135.56	151.70

E_a is higher in the presence of the inhibitors and increases with inhibitor's concentration. This implies that the corrosion process is retarded by the inhibitors and the barrier to mild steel corrosion increases continuously as more inhibitor molecules are added to the corrosive medium.

Adsorption Isotherm

An adsorption isotherm provides information on the manner (physical or chemical) in which an inhibitor molecule interacts with mild steel surface. Relevant adsorption data in Table 1 were fitted into Langmuir, Temkin, Frumkin, and Freundlich adsorption models to determine

which of these models could best describe the interactions of DCSE and DBSE with mild steel surface. From the results obtained, the adsorption behaviours of DCSE and DBSE are best described by the Temkin isotherm both at 313 K and 343 K. Plots of this isotherm with R^2 values are graphically displayed in Figure 2. Larger R^2 values obtained at 343 K suggests that the inhibitor molecules behave more ideally at this temperature.

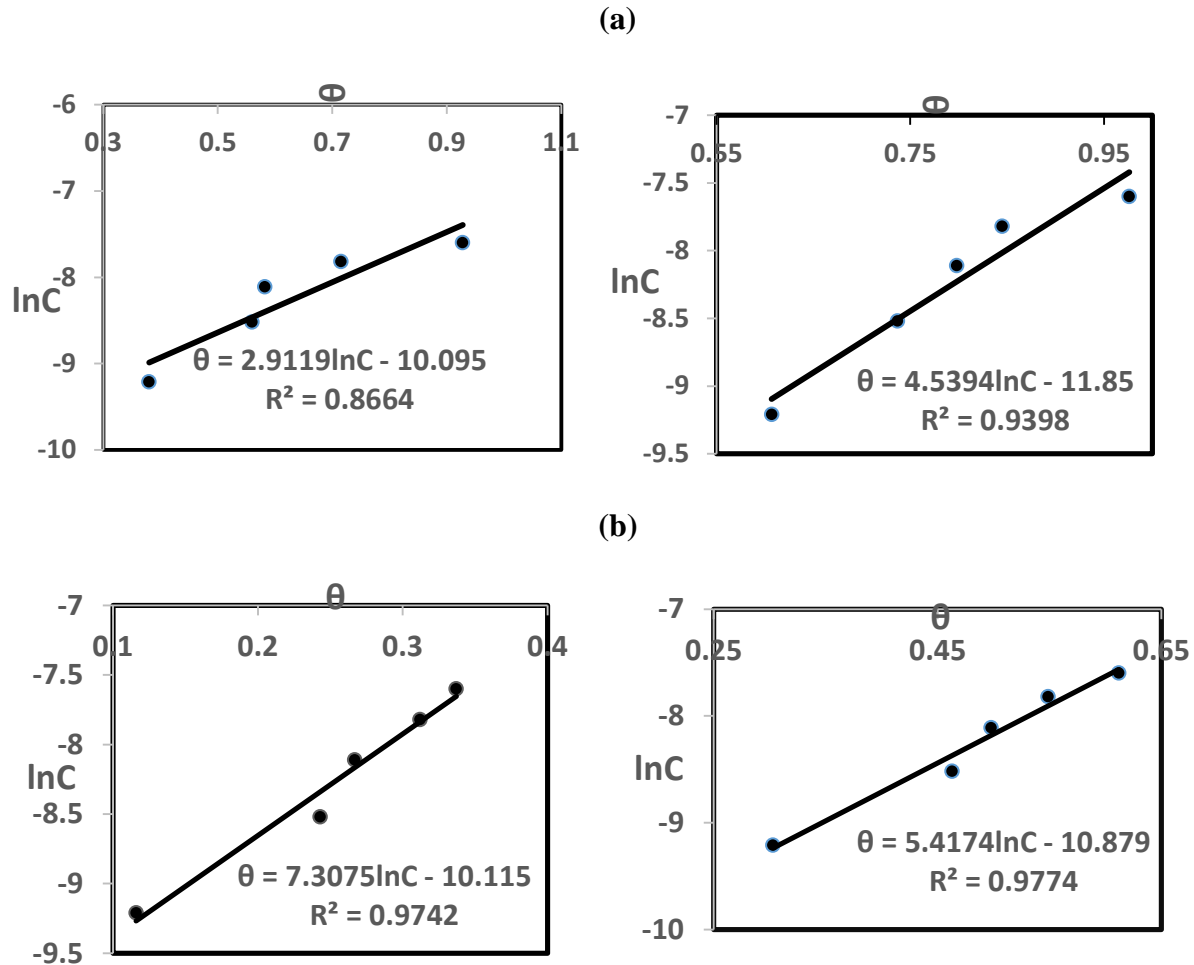


Figure 2: Temkin isotherm plots for adsorption of DCSE (left) and DBSE (right) onto mild steel at (a) 313 K and (b) 343 K.

The adsorption equilibrium constant (K_{ads}) values obtained from the isotherm plots are all less than unity (i.e. $K_{ads} < 1$). Consequently, the magnitude of the derived changes in adsorption free energy is small (Table 4) which signals the absence of chemical bond formation between the studied inhibitors and mild steel surface. Rather, the inhibitor molecules form a protective layer on the steel surface by means of physisorption as

reflected by their small negative ΔG_{ads} values. This mode of adsorption which involves electrostatic interaction between the inhibitors and mild steel surface is usually characterized by a $-\Delta G_{ads}$ value ≤ 20 kJmol^{-1} , unlike the chemisorption mode which is indicated by a $-\Delta G_{ads}$ value ≥ 40 kJmol^{-1} (Olasunkanmi *et al.*, 2021; Olasunkanmi *et al.*, 2020; Verma *et al.*, 2016).

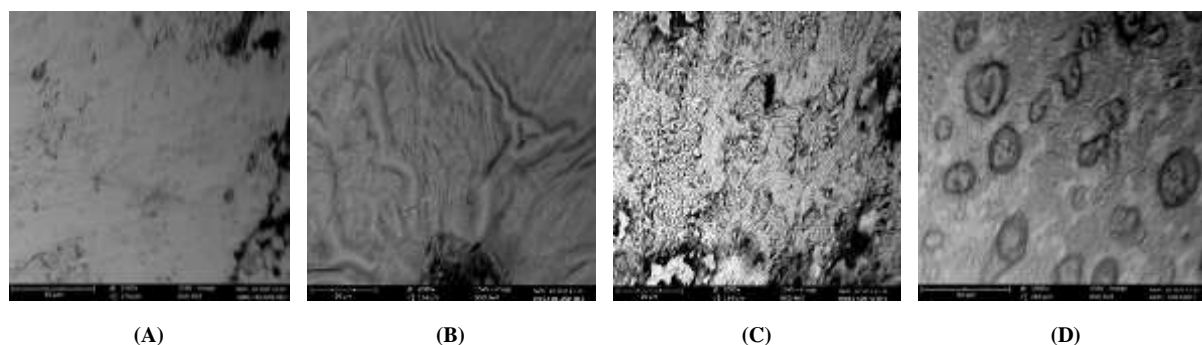
Table 4: K_{ads} and ΔG_{ads} values for adsorption of DCSE and DBSE onto mild steel in 1 M HCl at 313 K and 343 K

T(K)	$K_{\text{ads}} (\times 10^{-2})$		$\Delta G_{\text{ads}} (\text{kJmol}^{-1})$	
	DCSE	DBSE	DCSE	DBSE
313	3.12	19.77	-1.43	-6.23
343	10.77	13.43	-4.65	-5.23

Surface morphology study

Images of some corroded mild steel specimens from various corrosive media are shown in Figure 3 as revealed by scanning electron microscopy (SEM). Images A and B are the surfaces of corroded mild steel samples before and after immersion into 1 M HCl solution while

C and D are the surfaces after immersion into 1 M HCl solution containing 300 μM DCSE and 300 μM DBSE, respectively. Comparison of A, B, C and D shows that the corrosion of mild steel surface was successfully inhibited due to formation of protective layers of DCSE and DBSE on the metal surface.

**Figure 3:** SEM micro-graphs of mild steel surfaces before immersion (A) and after immersion in 1 M HCl (B), 1 M HCl + 300 μM DCSE (C) and 1 M HCl + 300 μM DBSE (D) at 313 K.

DFT calculations

In a nonacidic medium, the synthesized Schiff bases exist in their neutral forms, DCSE and DBSE. However, if they undergo protonation in HCl solution, the results are the doubly protonated forms, DCSE- 2H^+ and DBSE- 2H^+ , respectively. Therefore, both the neutral and protonated forms of the Schiff base compounds were fully optimized, giving the geometries shown in Table 5 with their respective HOMO and LUMO charge density maps. The obvious structural difference observed between the protonated and neutral forms may be ascribed to the electrostatic repulsion between the two positively charged iminium nitrogen ($-\text{C}=\text{NH}^+-$) of the protonated structures being greater than the lone pair-lone pair repulsion

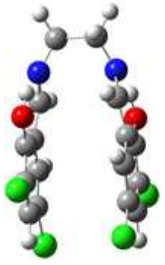
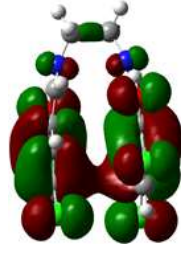
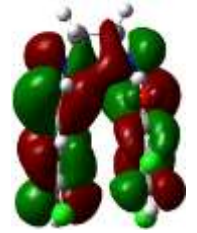
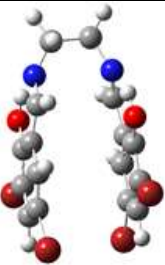
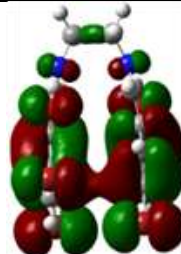
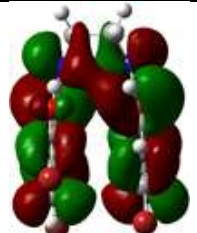
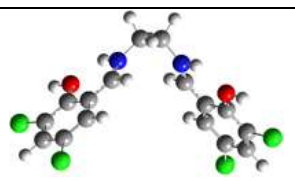
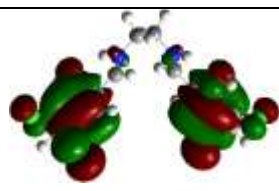
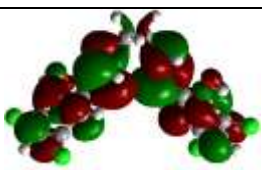
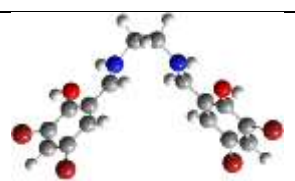
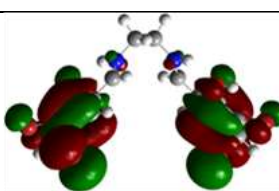
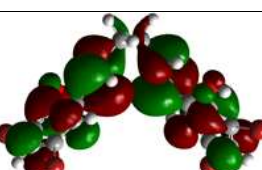
between the two-imine nitrogen ($-\text{C}=\text{N}-$) of the neutral structures.

The HOMO density map reveals the part of the Schiff base compounds that might be involved in charge donation to mild steel surface while the LUMO density map shows the portion that might be responsible for charge reception from the steel surface for the formation of protective layer. From the results presented in Table 5, nearly every part of the neutral species will be involved in charge exchange with mild steel surface unlike their protonated counterparts where the ethylene and iminium portions appear to be charge-deficient and will consequently not participate in charge donation to the steel face. In other words, only the substituted phenyl portion of the protonated species can release

charges to mild steel for interaction whereas the entire part of these species can receive incoming

charges from the metal surface as indicated by their LUMO density map.

Table 5: Optimized geometries of neutral and protonated forms of DCSE and DBSE with their respective HOMO and LUMO charge density maps.

Species	Optimized geometry	HOMO density map	LUMO density map
DCSE			
DBSE			
DCSE-2H ⁺			
DBSE-2H ⁺			

To account for the observed disparity in corrosion inhibition performance between DCSE and DBSE from quantum chemical point of view, the Schiff bases were compared based on selected reactivity descriptors derived from frontier molecular orbital energies (i.e. HOMO and LUMO energies). These descriptors were computed for both the neutral and protonated forms of the compounds as listed in Table 6.

E_{LUMO} and E_{HOMO} are descriptors that reveal the ease of receiving and donating electrons, respectively. Thus, these parameters show that DBSE has greater chance of donating to mild steel surface than DCSE which reflects the trend of inhibition efficiency.

Energy gap (Δ) and softness (σ) are indicative of overall reactivity and vulnerability to electron loss or change in electron density. The smaller the energy gap, the softer and more reactive is

the molecule. These descriptors therefore show that DBSE is more reactive and softer than DCSE, both in vacuum and acidic medium, neutral and protonated states.

Similarly, chemical potential (Φ) which reflects the ability to release electron reveals that DBSE has more electron donating power than DCSE both in neutral and protonated forms.

ΔN i.e. fraction of electron transferred is a descriptor that reveals the manner in which electrons were exchanged between an inhibitor molecule and mild steel surface. Positive ΔN (i.e. $\Delta N > 0$) indicates the movement of electrons

from the inhibitor to mild steel while negative ΔN (i.e. $\Delta N < 0$) implies that electrons migrate from mild steel to the inhibitor. In Table 6, ΔN values for the neutral form of the inhibitors imply that the movement of electrons is from the inhibitor to mild steel while the reverse is the case for the protonated form. The fact that more electrons were transferred to mild steel by DBSE (and less electron migrated to its protonated form from the steel) as suggested by its ΔN values explains why its inhibition efficiency is higher than that of DCSE.

Table 7: DFT-derived reactivity descriptors for the neutral and protonated forms of DCSE and DBSE both in vacuum and simulated HCl medium

Species	Descriptors					
	E_{LUMO} (eV)	E_{HOMO} (eV)	Δ (eV)	σ (eV)	Φ (eV)	ΔN (eV)
In-vacuo						
DCSE	-0.494	-8.439	7.945	0.252	-4.466	0.023
DBSE	-0.485	-8.361	7.876	0.254	-4.423	0.026
In simulated HCl medium						
DCSE	-0.328	-8.468	8.140	0.246	-4.398	0.027
DBSE	-0.326	-8.403	8.077	0.248	-4.364	0.030
[DCSE-2H⁺]	-1.922	-9.363	7.441	0.269	-5.642	-0.056
[DBSE-2H⁺]	-1.907	-9.231	7.324	0.273	-5.569	-0.051

Monte-Carlo simulations

The results of Monte-Carlo single molecule adsorption study between Fe (1 1 0) surface and the inhibitors are displayed in Figure 4 with their respective calculated adsorption energies (E_{ads}). These results show that the adsorption of DBSE and DCSE on Fe (1 1 0) surface is favoured by negative E_{ads} values which further indicate that DBSE, with a more negative adsorption energy, is more strongly attached to the surface. This

might explain why DBSE produced a greater corrosion inhibition effect on mild steel than DCSE as revealed by the inhibition efficiency data (Table 1). The very perfect planar shape of the inhibitor molecules on the Fe (1 1 0) surface (Figure 4) confirms the prediction of DFT that every part of each neutral molecule will be involved in the interaction with mild steel surface.

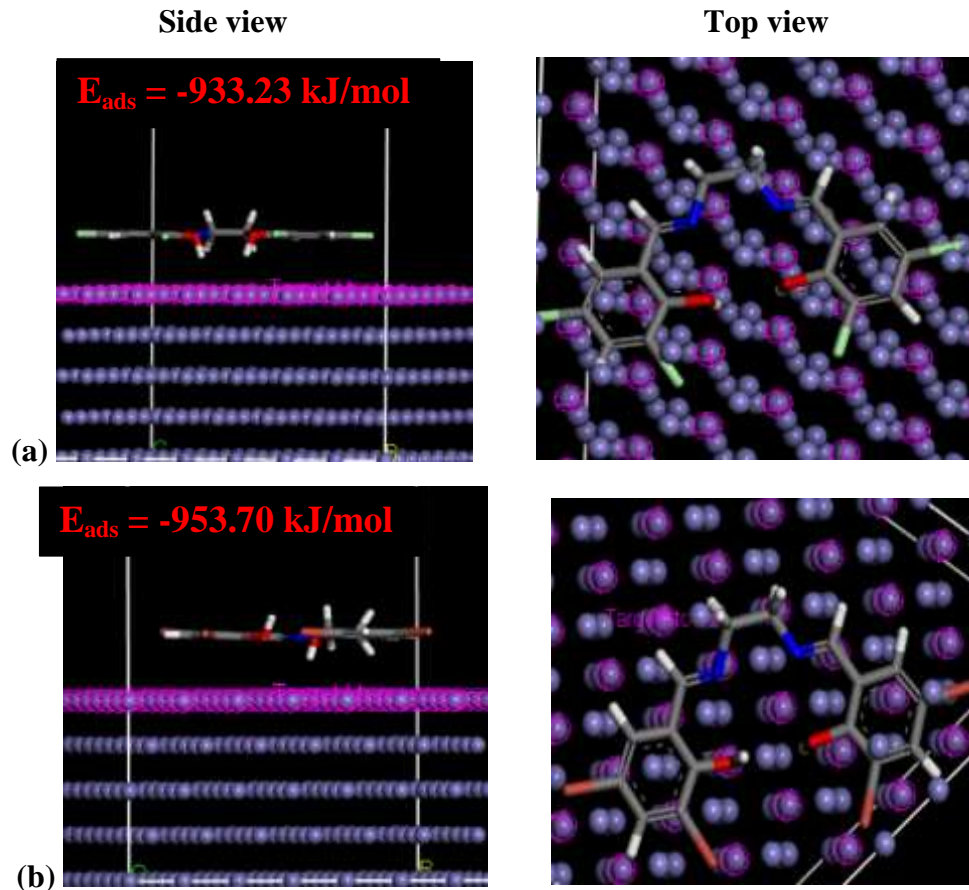


Figure 4: Monte-Carlo simulation of adsorption of DCSE (a) and DBSE (b) molecules on Fe (1 1 0) surface.

CONCLUSION

Bis(3,5-dichlorosalicylaldehyde) ethylenediamine (DCSE) and bis(3,5-dibromosalicylaldehyde) ethylenediamine (DBSE) have successfully been synthesized, characterized, and assessed as inhibitors of mild steel corrosion in 1 M HCl solution. The synthesized compounds inhibited mild steel corrosion in acidic medium, and the inhibition efficiency increased with concentration but decreased with temperature. Adsorption of DCSE and DBSE molecules at mild steel/HCl interface was best described by the Temkin adsorption model, with clear evidence favoring physisorption as the preferred mode of

adsorption. Inhibition efficiency rating was found as DBSE > DCSE and was traceable to difference in molecular size and electronegativity of the compounds. All experimental findings were strongly corroborated by the results of DFT and Monte Carlo calculations. We conclude that both DCSE and DBSE are viable candidates for effective mitigation of mild steel corrosion especially at low to moderately high temperatures.

ACKNOWLEDGEMENT

Authors appreciate the Centre for High-Performance Computing (CHPC), Cape Town, South Africa for providing access to the resources used for the computational study.

REFERENCES

- Abeng, F., Idim, V., Obono, O., & Magu, T. O. (2017). Adsorption and adsorption isotherm: application to corrosion inhibition studies of mild steel in 2 M HCl. *World Scientific News*, 77(2), 298-313.
- Akkermans, R. L., Spenley, N. A., & Robertson, S. H. (2013). Monte Carlo methods in materials studio. *Molecular Simulation*, 39(14-15), 1153-1164.
- Al-Baghdadi, S., Gaaz, T., Al-Adili, A., Al-Amiery, A., & Takriff, M. (2021). Experimental studies on corrosion inhibition performance of acetylthiophene thiosemicarbazone for mild steel in HCl complemented with DFT investigation. *International Journal of Low-Carbon Technologies*, 16(1), 181-188.
- Anderson, A. B., & Mehandru, S. (1984). Acetylene adsorption to Fe (100),(110), and (111) surfaces; structures and reactions. *Surface science*, 136(2-3), 398-418.
- Arya, A., & Carter, E. A. (2004). Structure, bonding, and adhesion at the ZrC (1 0 0)/Fe (1 1 0) interface from first principles. *Surface science*, 560(1-3), 103-120.
- Assad, H., & Kumar, A. (2021). Understanding functional group effect on corrosion inhibition efficiency of selected organic compounds. *Journal of Molecular Liquids*, 344, 117755.
- Basiony, N. E., Elgendy, A., Nady, H., Migahed, M., & Zaki, E. (2019). Adsorption characteristics and inhibition effect of two Schiff base compounds on corrosion of mild steel in 0.5 M HCl solution: experimental, DFT studies, and Monte Carlo simulation. *RSC advances*, 9(19), 10473-10485.
- Berisha, A. (2020). Experimental, Monte Carlo and molecular dynamic study on corrosion inhibition of mild steel by pyridine derivatives in aqueous perchloric acid. *Electrochem*, 1(2), 188-199.
- Boughoues, Y., Benamira, M., Messaadia, L., Bouider, N., & Abdelaziz, S. (2020). Experimental and theoretical investigations of four amine derivatives as effective corrosion inhibitors for mild steel in HCl medium. *RSC advances*, 10(40), 24145-24158.
- Brycki, B. E., Kowalczyk, I. H., Szulc, A., Kaczerewska, O., & Pakiet, M. (2018). Organic corrosion inhibitors. *Corrosion inhibitors, principles and recent applications*, 3, 33.
- Chai, J.-D., & Head-Gordon, M. (2008). Systematic optimization of long-range corrected hybrid density functionals. *The Journal of chemical physics*, 128(8), 084106.
- Chitra, S., Parameswari, K., Sivakami, C., & Selvaraj, A. (2010). Sulpha Schiff Bases as corrosion inhibitors for mild steel in 1M sulphuric acid. *Chemical Engineering Research Bulletin*, 14(1), 1-6.
- Clark, T., Chandrasekhar, J., Spitznagel, G. W., & Schleyer, P. V. R. (1983). Efficient diffuse function-augmented basis sets for anion calculations. III. The 3-21+ G basis set for first-row elements, Li-F. *Journal of Computational Chemistry*, 4(3), 294-301.
- Da Silva, A. B., D'Elia, E., & Gomes, J. A. d. C. P. (2010). Carbon steel corrosion inhibition in hydrochloric acid solution using a reduced Schiff base of ethylenediamine. *Corrosion science*, 52(3), 788-793.
- Ebrahimi, H. P., Hadi, J. S., Abdalnabi, Z. A., & Bolandnazar, Z. (2014). Spectroscopic, thermal analysis and DFT computational studies of salen-type Schiff base complexes. *Spectrochimica Acta Part A: Molecular and Biomolecular Spectroscopy*, 117, 485-492.
- Eddy, N., Ekwumemgbo, P., & Odoemelam, S. (2008). Inhibition of the corrosion of mild steel in H₂SO₄ by 5-amino-1-cyclopropyl-7-[(3R, 5S) 3, 5-dimethylpiperazin-1-YL]-6, 8-difluoro-4-oxo-quinoline-3-carboxylic acid (ACPDQC). *International Journal of Physical Sciences*, 3(11), 275-280.
- El Ibrahim, B., & Guo, L. (2020). Azole-based compounds as corrosion inhibitors for

- metallic materials. *Azoles-Synthesis, Properties, Applications and Perspectives*.
- Es-Sounni, B., Nakkabi, A., Bouymajane, A., Elaaraj, I., Bakhouch, M., Filali, F. R., . . . Fahim, M. (2022). Synthesis, Characterization, Antioxidant and Antibacterial Activities of Six Metal Complexes Based Tetradentate Salen Type Bis-Schiff Base.
- Frisch, M., Trucks, G., Schlegel, H., Scuseria, G., Robb, M., Cheeseman, J., . . . Petersson, G. (2009). Gaussian 09 Revision A. 1, 2009. *Gaussian Inc. Wallingford CT, 139*.
- Frisch, M. J., Pople, J. A., & Binkley, J. S. (1984). Self-consistent molecular orbital methods 25. Supplementary functions for Gaussian basis sets. *The Journal of chemical physics*, 80(7), 3265-3269.
- Guo, L., Qi, C., Zheng, X., Zhang, R., Shen, X., & Kaya, S. (2017). Toward understanding the adsorption mechanism of large size organic corrosion inhibitors on an Fe (110) surface using the DFTB method. *RSC advances*, 7(46), 29042-29050.
- Haque, J., Verma, C., Srivastava, V., Quraishi, M., & Ebenso, E. E. (2018). Experimental and quantum chemical studies of functionalized tetrahydropyridines as corrosion inhibitors for mild steel in 1 M hydrochloric acid. *Results in Physics*, 9, 1481-1493.
- Jamil, D. M., Al-Okbi, A. K., Al-Baghdadi, S. B., Al-Amiery, A. A., Kadhim, A., Gaaz, T. S., . . . Mohamad, A. B. (2018). Experimental and theoretical studies of Schiff bases as corrosion inhibitors. *Chemistry Central Journal*, 12(1), 1-9.
- Kokalj, A. (2012). On the HSAB based estimate of charge transfer between adsorbates and metal surfaces. *Chemical Physics*, 393(1), 1-12.
- Lgaz, H., Salghi, R., Larouj, M., Elfaydy, M., Jodeh, S., Rouifi, Z., . . . Oudda, H. (2016). Experimental, theoretical and Monte Carlo simulation of quinoline derivative as effective corrosion inhibitor for mild steel in 1 M HCl. *J. Mater. Environ. Sci*, 7(12), 4471-4488.
- Li, X.-L., Xie, B., Feng, J.-S., Lai, C., Bai, X.-X., Li, T., . . . Gu, Y.-T. (2022). 2-Pyridinecarboxaldehyde-based Schiff base as an effective corrosion inhibitor for mild steel in HCl medium: Experimental and computational studies. *Journal of Molecular Liquids*, 345, 117032.
- Mrani, S., El Arrouji, S., Karrouchi, K., El Hajjaji, F., Alaoui, K., Rais, Z., & Taleb, M. (2018). Inhibitory performance of some pyrazole derivatives against corrosion of mild steel in 1.0 M HCl: Electrochemical, MEB and theoretical studies. *International Journal of Corrosion and Scale Inhibition*, 7(4), 542-569.
- Nigusso, K. N. First Principles and Monte Carlo Studies of Adsorption and Desorption Properties from Pd1- Xagx Surface Alloy. Available at SSRN 4079128.
- Nor Zaini Tan, N. A., & Mohd Shotor, S. N. (2022). Corrosion inhibition screening of bromosalen and bromosalen-Mn (II) complex by a weight loss method. *Journal of Academia*, 10, 1-10.
- Nwankwo, H. U., Olasunkanmi, L. O., & Ebenso, E. E. (2017). Experimental, quantum chemical and molecular dynamic simulations studies on the corrosion inhibition of mild steel by some carbazole derivatives. *Scientific reports*, 7(1), 1-18.
- Olasunkanmi, L. O., Aniki, N. I., Adekunle, A. S., Durosinmi, L. M., Durodola, S. S., Wahab, O. O., & Ebenso, E. E. (2021). Investigating the synergism of some hydrazinecarboxamides and iodide ions as corrosion inhibitor formulations for mild steel in hydrochloric Acid: Experimental and computational studies. *Journal of Molecular Liquids*, 343, 117600.
- Olasunkanmi, L. O., Idris, A. O., Adewole, A. H., Wahab, O. O., & Ebenso, E. E. (2020). Adsorption and corrosion inhibition potentials of salicylaldehyde-based Schiff bases of semicarbazide and p-toluidine on mild steel in acidic

- medium: experimental and computational studies. *Surfaces and Interfaces*, 21, 100782.
- RAVARI, F., Dadgarinezhad, A., & Shekhshoei, I. (2009). Investigation on two salen type schiff base compounds as corrosion inhibition of copper in 0.5 M H₂SO₄. *Gazi University Journal of Science*, 22(3), 175-182.
- Resen, A., Hanoon, M., Alani, W., Kadhim, A., Mohammed, A., Gaaz, T., . . . Takriff, M. (2021). Exploration of 8-piperazine-1-ylmethylumbelliferone for application as a corrosion inhibitor for mild steel in hydrochloric acid solution. *International Journal of Corrosion and Scale Inhibition*, 10(1), 368-387.
- Seifzadeh, D., Valizadeh-Pashabeigh, V., & Bezaatpour, A. (2016). 5-CM-Salophen Schiff base as an effective inhibitor for corrosion of mild steel in 0.5 M HCl. *Chemical Engineering Communications*, 203(10), 1279-1287.
- Studio, A. D. 1.7, Accelrys Software Inc., San Diego, CA, USA. 2006.
- Sulaiman, K. O., & Onawole, A. T. (2016). Quantum chemical evaluation of the corrosion inhibition of novel aromatic hydrazide derivatives on mild steel in hydrochloric acid. *Computational and Theoretical Chemistry*, 1093, 73-80.
- Umoren, S. A., & Solomon, M. M. (2017). Synergistic corrosion inhibition effect of metal cations and mixtures of organic compounds: a review. *Journal of environmental chemical engineering*, 5(1), 246-273.
- Verma, C., Olasunkanmi, L. O., Bahadur, I., Lgaz, H., Quraishi, M., Haque, J., . . . Ebenso, E. E. (2019). Experimental, density functional theory and molecular dynamics supported adsorption behavior of environmental benign imidazolium based ionic liquids on mild steel surface in acidic medium. *Journal of Molecular Liquids*, 273, 1-15.
- Verma, C., Olasunkanmi, L. O., Ebenso, E. E., Quraishi, M. A., & Obot, I. B. (2016). Adsorption behavior of glucosamine-based, pyrimidine-fused heterocycles as green corrosion inhibitors for mild steel: experimental and theoretical studies. *The Journal of Physical Chemistry C*, 120(21), 11598-11611.
- Verma, C., & Quraishi, M. (2021). Recent progresses in Schiff bases as aqueous phase corrosion inhibitors: Design and applications. *Coordination Chemistry Reviews*, 446, 214105.
- Wahab, O. O., Olasunkanmi, L. O., Govender, K. K., & Govender, P. P. (2020). Tuning the aqueous solubility, chemical reactivity and absorption wavelength of azo dye through systematic adjustment of molecular charge density: a DFT study. *Molecular Physics*, 118(5), e1626508.
- Waziri, I., Kelani, M. T., Oyedeji-Amusa, M. O., Oyebamiji, A. K., Coetzee, L.-C. C., Adeyinka, A. S., & Muller, A. J. (2023). Synthesis and computational investigation of N, N-dimethyl-4-[(Z)-(phenylimino) methyl] aniline derivatives: Biological and quantitative structural activity relationship studies. *Journal of Molecular Structure*, 1276, 134756.
- Waziri, I., Mala, G. A., Wakil, I. M., Coetzee, L.-C. C., & Garba, H. Template Synthesis of Ni (II) and Zn (II) Complexes Derived from N₂O₂ Donor Symmetrical Tetradentate Ligands System: Comparative Antioxidant, Xanthine inhibitory, and Computational Studies.
- Waziri, I., Wahab, O., Mala, G., Oselusi, S., Egieyeh, S., & Nasir, H. (2023). Zinc (II) complex of (Z)-4-((4-nitrophenyl) amino) pent-3-en-2-one, a potential antimicrobial agent: synthesis, characterization, antimicrobial screening, DFT calculation and docking study. *Bulletin of the Chemical Society of Ethiopia*, 37(3), 633-651.
- Waziri, I., Yusuf, T. L., Akintemi, E., Kelani, M. T., & Muller, A. (2023). Spectroscopic, crystal structure, antimicrobial and antioxidant evaluations of new Schiff base compounds: An experimental and theoretical study. *Journal of Molecular Structure*, 1273, 134382.

- Waziri, I., Yusuf, T. L., Zarma, H. A., Oselusi, S. O., Coetzee, L.-C. C., & Adeyinka, A. S. (2023). New Palladium (II) Complexes from Halogen Substituted Schiff Base Ligands: Synthesis, Spectroscopic, Biological Activity, Density functional theory, and Molecular Docking Investigations. *Inorganica Chimica Acta*, 121505.
- Zinad, D., Jawad, Q., Hussain, M., Mahal, A., Mohamed, L., & Al-Amiery, A. (2020).

Adsorption, temperature and corrosion inhibition studies of a coumarin derivatives corrosion inhibitor for mild steel in acidic medium: gravimetric and theoretical investigations. *International Journal of Corrosion and Scale Inhibition*, 9(1), 134-151.